Near-Zero *TCF* SH0 Plate Acoustic Wave Resonators Using 36° *YX*-$LiTaO_3/SiO_2$ Film

Shuxian Wu, Zonglin Wu, Hangyu Qian, Feihong Bao*, Feng Xu, and Jie Zou*
School of Information Science and Technology
Fudan University
Shanghai, China
*Email: baofh@fudan.edu.cn, jiezou@fudan.edu.cn

Gongbin Tang*
Institute of Novel Semiconductors
Shandong University
Jinan, China
*Email: gongbin.tang@sdu.edu

***Abstract*—This work proposes a zero-th shear horizontal (SH_0) plate acoustic wave (PAW) resonator based on 36° *Y*-cut lithium tantalate (LT) / silicon dioxide (SiO_2) thin film. By using multi-physics finite-element-analysis (FEA) simulations, the rotation angle of LT and the layer thicknesses are optimized for obtaining large effective electromechanical coupling coefficient (k^2_{eff}) and low temperature coefficient of frequency (*TCF*). The fabricated resonators yield a k^2_{eff} of 11.8% and a Bode-Q_{max} of 1795. Moreover, the measured temperature coefficient of frequency at anti-resonant frequency (TCF_{fp}) is -4.9 ppm/°C, indicating that a near-zero *TCF* is realized in this study. The demonstrated resonators are promising for low loss and temperature-stable acoustic devices in wireless communication system.**

Keywords—acoustic resonators; shear horizontal; lithium tantalate; plate waves; temperature coefficient of frequency.

I. Introduction

With the rapid popularization of the communication technology, there has been increased attention paid to the high-performance acoustic devices for on-chip filters [1]-[3]. Currently, surface acoustic wave (SAW) and bulk acoustic wave (BAW) technology have dominated the main market for radio frequency front-end (RFFE) filters. SAW resonators using bulk Lithium Niobate (LN) or Lithium Tantalate (LT) monocrystalline substrates have a low manufacturing cost, and the frequency is defined by electrode width [4], [5]. However, there are limited frequency scaling capability due to finite lithography resolution. BAW resonators such as using Aluminum nitride (AlN) can reach extremely high frequency because of high acoustic velocity [6], [7]. But the frequency is determined by the thickness of the piezoelectric layer, and the manufacturing process is relatively complicated.

As an alternative solution, LN-based thin film plate wave resonators employing either the symmetric/asymmetric Lamb modes (S_0, S_1, A_0, A_1, …) or the Shear-Horizontal modes (SH_0, SH_1, …) have emerged as a promising technology, as they can yield ultra-high electromechanical coupling coefficient [8]-[13]. M. Kadota demonstrated a first-order antisymmetric mode (A_1) mode resonator using a 395 nm *Z*-cut LN plate at 5.4 GHz, while the obtained *Q* was not high enough [10]. V. Plessky proposed a laterally-excited bulk-wave resonator (XBAR) using a *Z*-cut monocrystalline LN film with improved k^2_{eff} and *Q* [12]. The temperature coefficient of frequency (*TCF*) of the LN-based thin film resonator is commonly poor, since LN material possess a negative temperature coefficient. Recently, S. Tanaka proposed a high frequency SH_1 mode plate wave resonator on 63° *Y*-cut LT thin film [14]. The measured *TCFs* were from −67 ppm/°C to −38 ppm/°C that need to be improved further. To meet the challenge, a 0-th shear horizontal plate acoustic wave (SH_0-PAW) resonator using 36° *Y*-cut LT/SiO_2 film is proposed in this work, where the SiO_2 film is designed to improve the temperature stability of the devices.

II. Design and Simulations

Fig. 1(a) and (b) illustrates a schematic overview of the proposed SH_0-PAW resonator, including an IDT and two grating reflectors (GRs), a single crystal *Y*-cut LT thin film, a SiO_2 layer, and a supporting substrate. The IDT is placed in the middle of the resonator, and the GRs are placed on both sides of the IDT to ensure the wave reflection condition. There are two kinds of plate waves, the Lamb wave (S_0, A_0, S_1, A_1, …) or plate shear wave (SH_0, SH_1, …). Among all the plate modes, SH_0 mode presents a superiority of interdigital-transducer (IDT) in frequency definition due to slow dispersion [15]. The suspended plate structure prevents acoustic energy leakage. In simulations, the aperture (W) of IDT is set to 0.1λ, and the width (a) and pitch (p) of the electrode finger are set to $\lambda/4$ and $\lambda/2$, respectively. The value of p determines the acoustic wave wavelength ($\lambda = 2p$) and the resonant frequency, shown as follows,

$$f_r = \frac{v_0}{2p} \tag{1}$$

where v_0 represents the phase acoustic velocity with short-circuited electrodes. The rotation angle (θ) of LT is obtained by setting *ZXZ* Euler angles (0, 90 − θ°, 0). Periodic boundary conditions in propagation direction (*x*-direction) and shear horizontal direction (*y*-direction) are imposed to reduce the computation complexity. The k^2_{eff} of the resonator is calculated by the series-resonant frequency (f_s) and parallel-resonant frequency (f_p), shown as follows [16],

$$k^2_{eff} = \frac{\pi}{2}\frac{f_s}{f_p}\frac{1}{\tan(\frac{\pi}{2}\frac{f_s}{f_p})}, \tag{2}$$

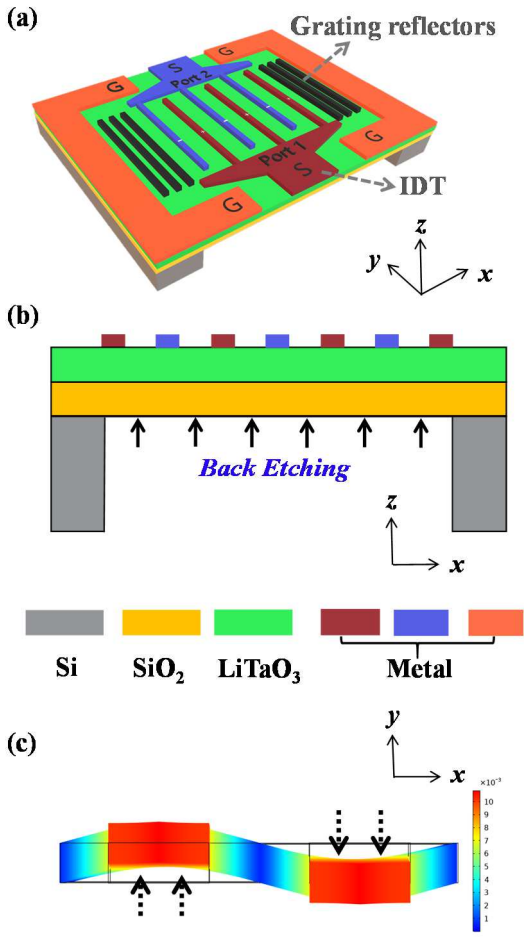

Fig. 1. (a) Diagram of 0-th shear horizontal plate acoustic waves (SH_0-PAWs) resonators. (b) Simulated displacement distribution of lateral excited SH_0 mode.

and the phase acoustic velocity (v_p) is calculated using the following formula: $v_p = f_p\lambda$.

In this work, a zero-th shear horizontal mode plate acoustic waves (SH_0-PAW) resonator using 36° *YX*-LT/SiO_2 thin film is proposed, where the SiO_2 layer with positive temperature coefficient is served as temperature compensation function. The displacements of SH_0 mode vibration using finite-element-analysis (FEA) method are shown in Fig. 1(c). It can be found that the vibration mainly focuses in shear horizontal direction (y), indicating that the SH_0 mode is y-direction polarization.

In Fig. 2, it shows the calculated k^2_{eff} and phase acoustic velocity (v_p) of resonators with different LT rotation angles. When the θ is around 30°, there are a k^2_{eff} and a high v_p. In this study, 36° is selected as the design value. In the case of $\theta = 36°$, the thicknesses of LT layer and SiO_2 layer (h_{LT} and h_{SiO2}) are optimized, and the contour map of k^2_{eff} is shown in Fig. 3. When the h_{LT} and h_{SiO2} are between 0.1λ and 0.4λ, it presents a large k^2_{eff}. To analyze the temperature stability of the resonators with different layer thicknesses, the temperature coefficients of frequency at series resonant frequency (TCF_{fs}) and parallel resonant frequency (TCF_{fp}) are calculated, listed in TABLE I. When the h_{LT} and h_{SiO2} are 0.2λ, the TCF_{fp} is near-zero about

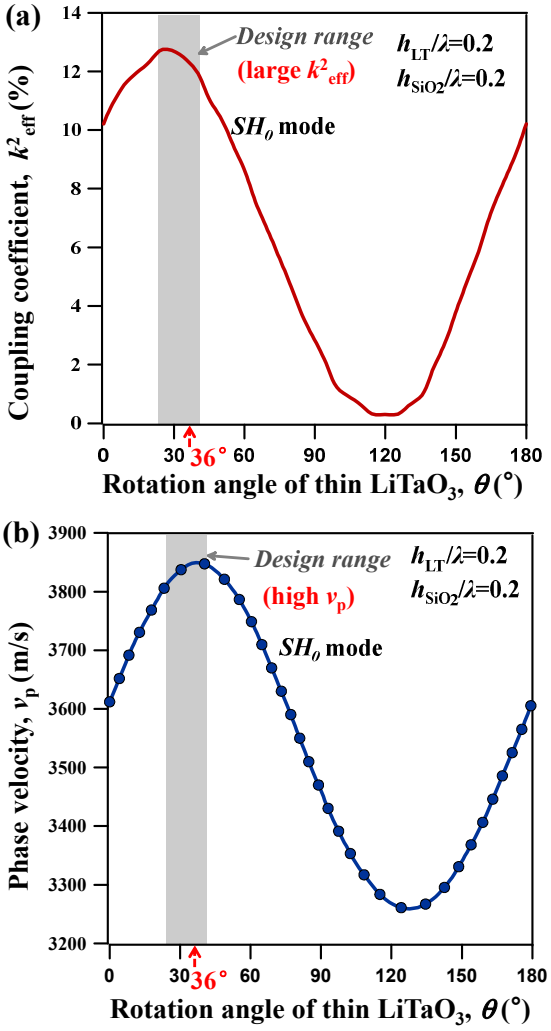

Fig. 2. (a) k^2_{eff} and (b) v_p vary with the rotation angles of $LiTaO_3$ thin film. When the θ is around 30°, there are a k^2_{eff} and a high v_p. In this study, 36° is selected as the design value of the rotation angles.

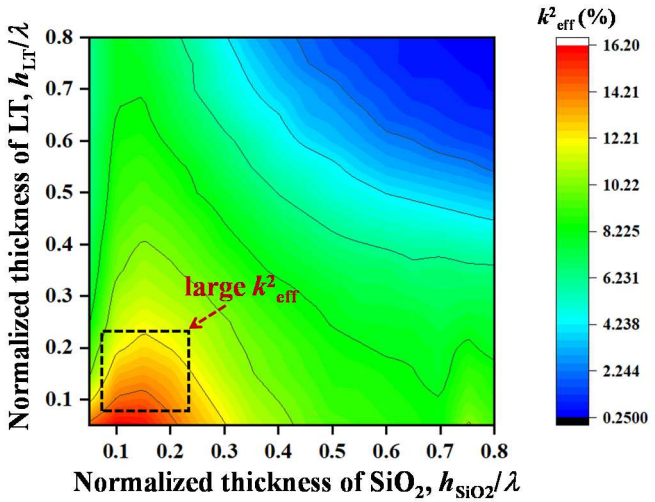

Fig. 3. The contour map of k^2_{eff} varies with different h_{LT}/λ and h_{SiO2}/λ when the rotation angle of LT is 36°. It can be found that there is a large k^2_{eff} when the h_{LT} and h_{SiO2} are between 0.1λ and 0.4λ.

TABLE I. THE CALCULATED TCF_{FP} OF THE RSONATORS (PPM/°C)

	$h_{LT}=0.1\lambda$	$h_{LT}=0.2\lambda$	$h_{LT}=0.3\lambda$	$h_{LT}=0.4\lambda$
$h_{SiO2}=0.1\lambda$	-9.7	-24.2	/	/
$h_{SiO2}=0.2\lambda$	9.7	**-3.3**	-20.3	-25.1
$h_{SiO2}=0.3\lambda$	/	4.2	-4.6	/
$h_{SiO2}=0.4\lambda$	/	17.2	/	10.2

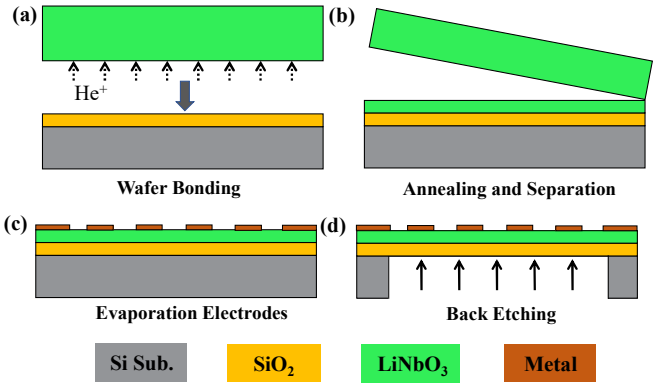

Fig. 4. Fabrication process. (a) A single crystal LN wafer implanted by He ions (He^+) is bonded to a thermally oxidized Si substrate. (b) The thick LN substrates are separated after being placed in the annealing furnace. (c) The electrodes are formed using lift-off process. (d) Si substrates are removed by ICP back etching from the bottom.

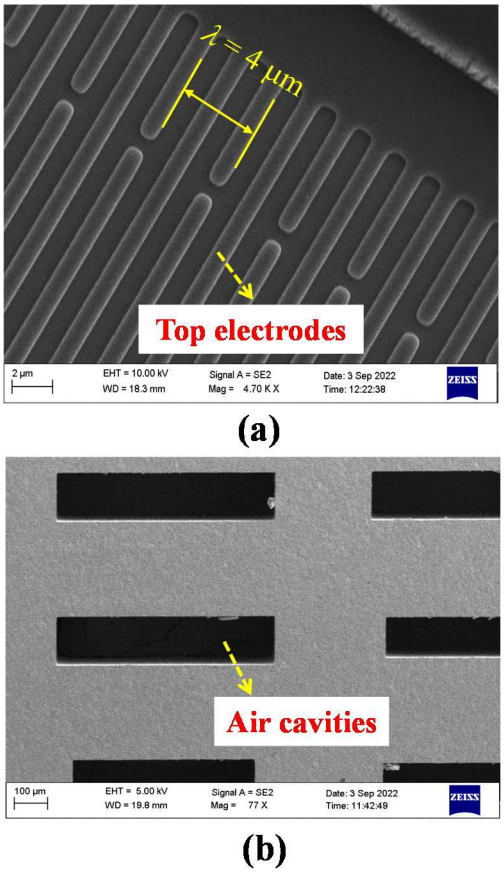

Fig. 5. SEM images of fabricated PAWs resonators. (a) Topography of the top electrodes. (b) Air cavities of the fabricated resonators from the bottom view.

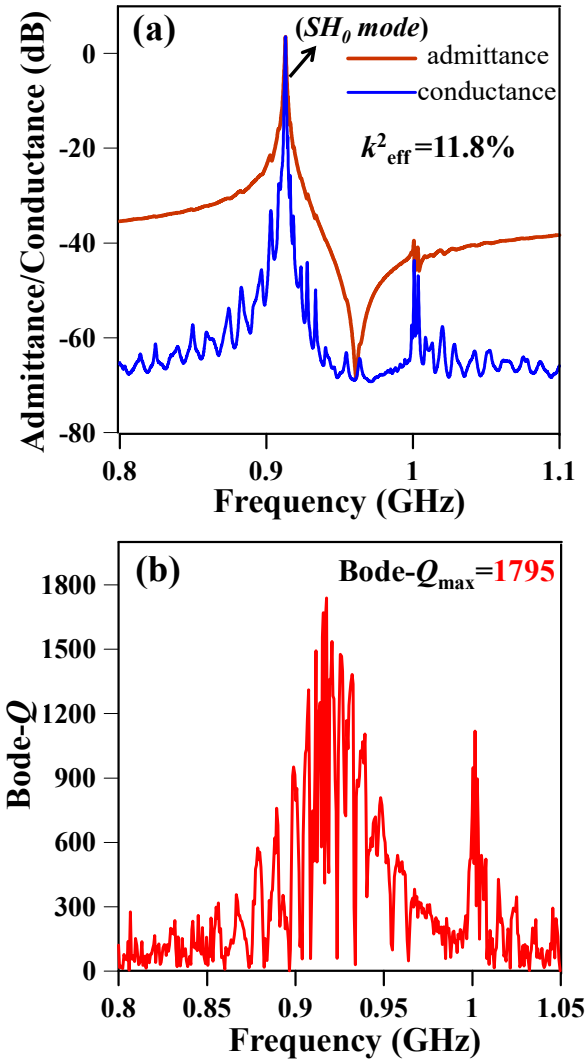

Fig. 6. (a) Measured admittance/conductance responses of SH_0 PAWs resonators. (b) Measured Bode-Q curve of resonators.

-3.3 ppm/°C. Thus, the thicknesses of LT layer and SiO_2 layer are designed as 0.2λ.

III. FABRICATION AND MEASUREMENT RESULTS

The proposed resonators are manufactured by using smart-cut technology, including ions implantation, wafer bonding, lift-off, and back etching, as shown in Fig. 4. Firstly, Helium ions (He^+) was implanted into a single crystal LN wafer, and then the LN wafer was bonded to a thermally oxidized Si substrate. Secondly, the bonded wafer is patterned by ultraviolet lithography, and the Aluminum (Al) and Titanium (Ti) metals were evaporated on the top of the wafer. Thirdly, the electrode fingers were formed by using lift-off process. Finally, the Si substrate on the back was removed by inductively coupled plasmas (ICP) etching using Bosch process.

The S-parameters of the fabricated devices are measured by a GSG probe and a vector network analyzer. Using a scanning electron microscope (SEM), the top electrodes and the bottom

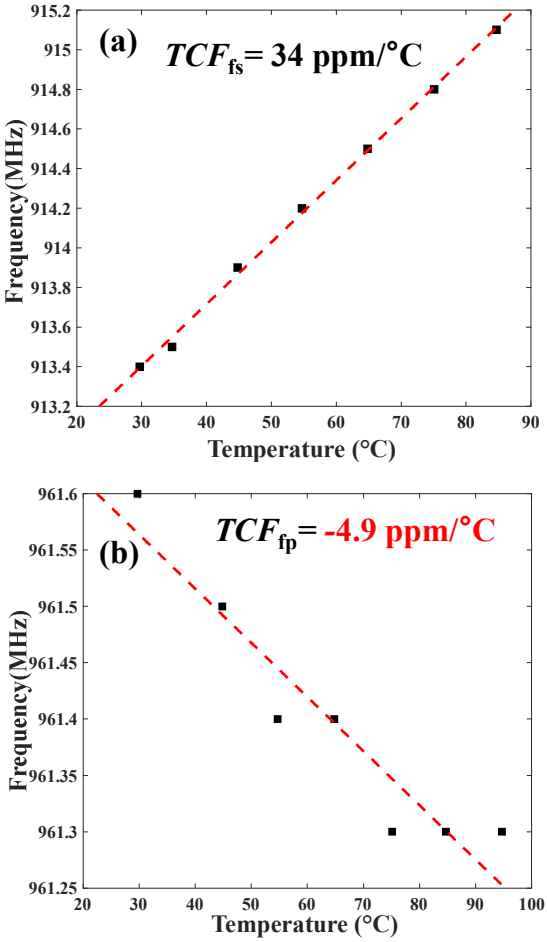

Fig. 7. (a) Measurement results of frequencies vary with temperatures. (a) Temperature coefficient of frequency at resonant frequency (TCF_{fs}). (b) Temperature coefficient of frequency at anti-resonant frequency (TCF_{fp}).

cavities of resonators are observed, as shown in Fig. 5. It can be found that the morphology of the electrodes is visibly clear, and the perpendicularity of the cavities is excellent.

Then, the measurement results of the resonators are analyzed. The k^2_{eff} and Bode-Q are extracted, shown in Fig. 6. The Bode-Q is defined as follows [17]:

$$\text{Bode-}Q(f) = 2\pi f \frac{|S_{11}|}{1-|S_{11}|^2}\tau(S_{11}), \tag{3}$$

where f represents the frequency, and $\tau(S_{11})$ represents the group delay of S_{11}. It shows that the fabricated resonators yield a k^2_{eff} of 11.8%, a Bode-Q_{max} of 1795, and a figure of merit (FoM = k^2_{eff}·Bode-Q_{max}) of 212, which is higher than most PAW resonators.

Moreover, the $TCFs$ of the resonators are measured at different temperature condition, shown in Fig. 7. The measured TCF_{fs} and TCF_{fp} are 34 ppm/°C and -4.9 ppm/°C, respectively. Simulation and measurement results verified a near-zero TCF_{fp} of LT-based PAW resonator, suggesting that the proposed resonator has an excellent temperature stability at parallel-resonant frequency. The TCF_{fp} is one of the very important parameters which determines the robustness of the device's frequency at different temperature environment.

IV. Conclusions

In this paper, a SH_0-PAW resonator using 36° YX-LT/SiO_2 thin film is designed and fabricated. For improving k^2_{eff} and TCF of the resonators, the rotation angle of LT is designed as 36°, and both the thicknesses of LT layer and SiO_2 layer are optimized as 0.2λ. The measurement results of fabricated resonators show a k^2_{eff} of 11.8%, a Bode-Q_{max} of 1795, and a TCF_{fp} of – 4.9 ppm/°C. The proposed resonators show a relatively large k^2_{eff}, a high Q and a near-zero TCF_{fp}, providing an effective solution for designing high-performance and CMOS-compatible acoustic filters and oscillators. Reducing the gap between TCF_{fs} and TCF_{fp} of the resonators will be one of our next works.

References

[1] S. Parkvall, E. Dahlman, A. Furuskar, and M. Frenne, "NR: The new 5G radio access technology," *IEEE Commun. Standards Mag.*, vol. 1, no. 4, pp. 24–30, Dec. 2017.

[2] R. Aigner, G. Fattinger, M. Schaefer, K. Karnati, R. Rothemund, and F. Dumont, "BAW filters for 5G bands," *in IEDM Tech. Dig.*, Dec. 2018, pp. 1–5.

[3] C. C. W. Ruppel, "Acoustic wave filter technology—A review," *IEEE Trans. Ultrason., Ferroelectr., Freq. Control*, 2017. vol. 64, no. 9, pp. 1390–1400, Sep. 2017.

[4] M. Kadota and S. Tanaka, "Wideband acoustic wave resonators composed of hetero acoustic layer structure," *Japanese J. Appl. Phys.*, vol. 57, no. 7S1, Jul. 2018, Art. no. 07LD12.

[5] J. Shen, S. Fu, R. Su, H. Xu, Z. Lu, Z. Xu, J. Luo, F. Zeng, C. Song, W. Wang, and F. Pan, "High-performance surface acoustic wave devices using $LiNbO_3$/SiO_2/SiC multilayered substrates," *IEEE Trans. Microw. Theory Techn.*, vol. 69, no. 8, pp. 3693–3705, Aug. 2021.

[6] J. Yang, X. -Q. Jiao, R. Zhang, H. Zhong and Y. Shi, "Fabrication of bulk acoustic wave resonator based on AlN thin film," *2012 Symposium on Piezoelectricity, Acoustic Waves, and Device Applications (SPAWDA)*, 2012, pp. 191-194.

[7] R. Ruby, "Review and comparison of bulk acoustic wave FBAR, SMR technology," in *Proc. IEEE Int. Ultrason. Symp.*, New York, NY, USA, Oct. 2007, pp. 1029–1040.

[8] T. Kimura, M. Omura, Y. Kishimoto, and K. Hashimoto, "Comparative Study of Acoustic Wave Devices Using Thin Piezoelectric Plates in the 3–5 GHz Range," *IEEE Trans. Microwave Theory Techn.*, vol. 67, no. 3, pp. 915–921, Mar. 2019.

[9] M. Bousquet, P. Perreau, C. MaederPachurka, A. Joulie, F. Delaguillaumie, J. Delprato, G. Enyedi, G. Castellan, C. Eleouet, T. Farjot, C. Billard, and A. Reinhardt, "Lithium niobate film bulk acoustic wave resonator for sub-6 GHz filters", *Proceedings of the 2020 IEEE International Ultrasonics Symposium (IUS)*, vol. pp. 2020.

[10] M. Kadota and T. Ogami, "5.4 GHz Lamb wave resonator on $LiNbO_3$ thin crystal plate and its application," *Jpn. J. Appl. Phys.*, vol. 50, no. 7, p. 07HD11, Jul. 2011.

[11] Y. Yang, A. Gao, R. Lu, and S. Gong, "5 GHz lithium niobate MEMS resonators with high FoM of 153," in *Proc. IEEE 30th Int. Conf. Micro Electro Mech. Syst. (MEMS)*, Jan. 2017, pp. 942–945.

[12] V. Plessky, S. Yandrapalli, P. J. Turner, L. G. Villanueva, J. Koskela, and R. B. Hammond, "5 GHz laterally-excited bulk-wave resonators (XBARs) based on thin platelets of lithium niobate," *Electronics Letters*, vol. 55, no. 2, pp. 98–100, 2019.

[13] S. Yandrapalli, S. E. K. Eroglu, V. Plessky, H. B. Atakan, and L. G. Villanueva, "Study of Thin Film $LiNbO_3$ Laterally Excited Bulk Acoustic

Resonators," *Journal of Microelectromechanical Systems*, vol. 31, no. 2, pp. 217–225, Jan. 2022.

[14] F. Setiawan, M. Kadota, S. Tanaka. "2E2-1 High-Frequency SH_1 Mode Plate Wave Resonator on $LiTaO_3$ Using Aluminum as Backside Electrode[C]"//*Proceedings of Symposium on Ultrasonic Electronics. Institute for Ultrasonic Elecronics*, 2022, 43: 313.

[15] J. Zou, V. Yantchev, F. Iliev, V. Plessky, S. Samadian, R. B. Hammond, and P. J. Turner, "Ultra-Large-Coupling and Spurious-Free SH_0 Plate Acoustic Wave Resonators Based on Thin $LiNbO_3$," *IEEE Trans. Ultrason. Ferroelect. Freq. Control*, vol. 67, no. 2, pp. 374–386, Feb. 2020.

[16] R. Aigner, Bringing BAW technology into volume production the ten commandments and the seven deadly sins, *Intl. Symp. Acoustic Wave Devices for Future Mobile Communication Systems*. (2007) 85.

[17] D. A. Feld, R. Parker, R. Ruby, P. Bradley, and S. Dong, "After 60 years: A new formula for computing quality factor is warranted," in *2008 IEEE Ultrasonics Symposium*, Beijing, China, Nov. 2008, pp. 431–436.